Journal of Quantitative Spectroscopy & Radiative Transfer 111 (2010) 1065–1079

Contents lists available at ScienceDirect

Journal of Quantitative Spectroscopy & Radiative Transfer

journal homepage: www.elsevier.com/locate/jqsrt

Measurement and computations for temperature dependences of self-broadened carbon dioxide transitions in the 30012←00001 and 30013←00001 bands

A. Predoi-Cross [a,*], W. Liu [a], R. Murphy [a], C. Povey [a], R.R. Gamache [c], A.L. Laraia [c], A.R.W. McKellar [b], D.R. Hurtmans [d], V. Malathy Devi [e]

[a] Department of Physics and Astronomy, University of Lethbridge, 4401 University Drive, Lethbridge, AB, Canada T1K 3M4
[b] Department of Environmental, Earth, and Atmospheric Sciences, University of Massachusetts Lowell, USA
[c] Steacie Institute for Molecular Sciences, National Research Council of Canada, Ottawa, ON, Canada
[d] Service de Chimie Quantique et Photophysique, Université Libre de Bruxelles, 50 Av F.D. Roosevelt, cp160/09, B-1050 Bruxelles, Belgium
[e] Department of Physics, The College of William and Mary, Williamsburg, VA, USA

ARTICLE INFO

Article history:
Received 16 November 2009
Received in revised form
6 January 2010
Accepted 11 January 2010

Keywords:
CO_2
Line broadening
Shifting and mixing
Fourier transform spectroscopy
Temperature dependences
Semi-classical calculations
Energy Corrected Sudden calculations

ABSTRACT

Using a Fourier transform spectrometer setup we have measured the self-broadened half width, pressure shift, and line asymmetry coefficients for transitions in the 30012←00001 and 30013←00001 vibrational bands of carbon dioxide for four different temperatures. A total of 46 pure CO_2 spectra were recorded at 0.008 and 0.009 cm^{-1} resolution and at pressures varying from a few Torr to nearly an atmosphere. The individual spectral line profiles have been fitted by a Voigt profile and a speed-dependent Voigt profile, to which we have added dispersion profiles to account for weak line mixing. A comparison of the sets of results obtained for each band showed no vibrational dependence of the broadening coefficients. The self-broadening and self-shift coefficients are compared to semiclassical calculations based on the Robert–Bonamy formalism and were found to be in good agreement. The line asymmetry results are compared to line mixing calculations based on the Energy Corrected Sudden (ECS) and Exponential Power Gap models.

1. Introduction

Carbon dioxide is a trace constituent of the Earth's atmosphere and is well mixed up to high altitudes. Over the past few hundreds of years the effects of human activities on our environment have escalated. It is believed that the anthropogenic emissions of greenhouse gases may cause changes in our global climate for many years to come. Recent scientific efforts to understand, quantify and predict the effects of human activities on Earth's atmosphere led to numerous studies of its main greenhouse gas, carbon dioxide [1 and reference therein].

As the remote sensing technology continues to improve, the quality of the spectroscopic data needed to interpret them has to follow the trend. Often, the laboratory studies try to reproduce the pressure and temperature ranges expected on the planetary atmosphere that is of interest. Our study is also relevant to present and future remote sensing studies of the planetary atmospheres of Mars and Venus [1 and reference therein]. For example, measurements of spectroscopic line parameters of carbon dioxide isotopologues are key to the accurate determination of CO_2 isotope ratios in the Martian atmosphere that will help scientists understand

* Corresponding author.
E-mail address: adriana.predoicross@uleth.ca (A. Predoi-Cross).

0022-4073/$ - see front matter © 2010 Elsevier Ltd. All rights reserved.
doi:10.1016/j.jqsrt.2010.01.003

its atmospheric evolution and search for evidence of biogenic activity.

Until recently, most of the studies reporting spectroscopic line parameters were based on fitting the profiles to Voigt or Lorentz line shapes. As shown in the room temperature measurements of pure carbon dioxide transitions in the two Fermi bands of interest in the present study [2–4], the Voigt profiles do not model accurately the observed absorption profiles. Often a better representation of the observed profiles is obtained when line mixing effects are accounted for. In this study we have followed this approach.

There have been very few studies on the temperature dependence of self broadening coefficients in carbon dioxide [5–11]. Fourier transform spectra recorded at 197, 233 and 294 K were used to study the temperature dependence of 22 self-broadened transitions in each of the 30013←00001 [5] and 30012←00001 [6] vibrational bands. The absolute line intensities, self- and foreign-gas broadened line parameters were retrieved using a Voigt profile. The authors compared their experimental results with earlier measurements by other investigators and with theoretical calculations of broadening parameters.

Diode laser spectroscopy was employed by Tettemer and Planet [7] to measure the line intensities, self- and N_2-broadened half width for 9 transitions in the v_2 band and 5 transitions in the $2v_2-v_2$ band of carbon dioxide. Those measurements were carried out over the 200–325 K temperature range. The reported temperature dependence exponents for all transitions were above 0.5.

Using a grating spectrometer Margottin-Maclou et al. [8] have measured the room temperature self-broadening parameters for 42 transitions in the v_3 band of CO_2. The N_2- and O_2-broadening parameters were measured at 296 and 198 K for transitions in the v_3 and v_1+v_3 bands. The authors compared their experimental results with semi-classical calculations.

Varanasi [9] published a comprehensive review of self-, N_2- and O_2-broadened carbon dioxide transitions belonging to selected mid-infrared vibrational bands. The measurements were performed in the 197–620 K temperature range. The experimental measurements were complemented by a discussion of the theoretical models available for calculations of collisional broadening coefficients. Aushev et al. [10] studied the CO_2 self-broadened spectra of six transitions in the v_3 band and four transitions in the laser band at very high temperatures (1000–3000 K). Arshinov and Leshenyuk [11] studied one self-broadened R branch transition belonging to the laser band in the 290–600 K range.

To a certain extent, the results presented here are complementary to our study of temperature dependences of air broadening coefficients for transitions in the 30012←00001 and 30013←00001 bands of carbon dioxide [12]. This is the first set of measurements for temperature dependences of self-broadening, self-induced pressure shifts and line mixing coefficients in these two bands. The Voigt and speed-dependent Voigt profiles with associated asymmetric components to account for line mixing effects were used to model the line shape profiles. The self-broadening coefficients and associated temperature dependence exponents were modeled using semi-classical calculations based on the Robert–Bonamy formalism [13]. The line mixing coefficients were compared with values calculated using the Energy Power Gap (EPG) and Energy Corrected Sudden (ECS) scaling laws. Overall, we observe a good agreement between the measurements and the corresponding theoretical calculations.

2. Experimental details and results

The spectra were recorded at the National Research Council of Canada using a Bomem DA3.002 Fourier transform spectrometer and a coolable multi-traversal absorption cell with a base length of 5 m, as described in our study of CO_2 + air mixtures [12]. In Table 1 we present a summary of the experimental conditions of all spectra used in this study. The nominal spectral resolution was either 0.008 cm^{-1} or 0.009 cm^{-1} and the total absorption path was either 20.15 or 40.15 m. Each spectrum was an average of 24–32 interferograms, representing a data acquisition time of approximately 2 h.

The absorption cell resides inside a vacuum jacket and the entire optical path outside the cell is evacuated. Cooling is accomplished by means of flowing liquid methanol from a refrigerated cooling bath through copper coils soldered to the outside of the cell. The gas temperature is monitored by platinum resistance thermometers mounted on the cooling lines and inside the cell, as well as from the temperature of the cooling bath itself. Gas pressures are measured with an estimated accuracy of about 0.3% using Baratron Model 127 capacitance manometers (with full scale ranges of 10 and 1000 Torr) and a Wallace and Tiernan Model FA145 Bourdon tube gauge.

A total of 28 cold spectra were analyzed, with sample pressures ranging from 7 to 665 Torr (1 Torr = 133.322 Pa) and sample temperatures of 218, 235, or 259 K. The rotational gas temperatures reported in Table 1 were determined using selected line intensities from our pure gas, room temperature study of these two bands [4]. The estimated accuracy of the temperature determination is ± 0.5 K, with a further uncertainty of ± 0.5 K due to possible variations along the 5 m length of the cell. The uncertainty and inhomogeneity are greatest at the lowest temperature (218 K). The analysis also incorporated 18 room temperature spectra used in [4].

The 46 self-broadened CO_2 spectra were divided into four sets according to the temperature at which they were recorded. The individual sets of spectra were analyzed using a multispectrum nonlinear least squares technique [14] to retrieve the line parameters at that temperature. Next, the temperature dependences of the broadening and shift coefficients were determined and compared. We attempted to retrieve the self-broadening, self-shift and line mixing coefficients for all pure carbon dioxide transitions in the 30013←00001 and 30012←00001 vibrational bands that were visible in our spectra. The line shape functions used were the Voigt and speed dependent Voigt convolved with the instrumental line shape appropriate for our instrument. During each fit, the

Table 1
Spectral conditions for the pure CO_2 spectra analyzed in this study.

Pressure (Torr)	Path length (m)	Temp. (K)	Res. (cm^{-1})	Pressure (Torr)	Path length (m)	Temp. (K)	Res. (cm^{-1})
8.3	40.15	293.9	0.008	503.0	20.15	258.8	0.009
9.5	40.15	293.9	0.008	657.0	20.15	258.8	0.009
60.0	60.15	294.1	0.008	6.6	40.15	235.1	0.009
60.2	40.15	294.0	0.008	8.0	20.15	235.1	0.009
99.5	40.15	294.2	0.008	43.3	40.15	235.1	0.009
123.7	40.15	293.8	0.008	74.3	20.15	235.1	0.009
150.1	80.15	294.2	0.008	85.0	40.15	235.1	0.009
200.0	40.15	293.9	0.008	159.0	40.15	235.1	0.009
201.0	60.15	294.3	0.008	159.0	20.15	235.1	0.009
300.5	40.15	294.2	0.008	251.0	20.15	235.1	0.009
301.0	80.15	294.6	0.008	266.0	40.15	235.1	0.009
400.6	40.15	294.0	0.008	370.0	20.15	235.1	0.009
501.3	40.15	294.5	0.008	401.0	40.15	235.1	0.009
502.0	60.15	295.0	0.009	501.0	40.15	235.1	0.009
600.3	40.15	294.2	0.008	538.0	20.15	235.1	0.009
699.0	60.15	294.6	0.009	664.0	40.15	235.1	0.009
701.0	60.15	295.1	0.009	8.1	20.15	217.6	0.009
701.5	40.15	294.6	0.008	68.4	20.15	217.6	0.009
7.2	20.15	258.8	0.009	122.1	20.15	217.6	0.009
57.2	20.15	258.8	0.009	175.3	20.15	217.6	0.009
110.3	20.15	258.8	0.009	265.3	20.15	217.6	0.009
199.0	20.15	258.8	0.009	400.5	20.15	217.6	0.009
357.5	20.15	258.8	0.009	506.4	20.15	217.6	0.009

analysis software was modeling the spectral backgrounds and zero transmission levels.

As in our room temperature study [4], the groups of spectra recorded at the same temperature were divided in sections of about 2–3 cm^{-1} wide and analyzed using the multispectrum analysis software. The initial values for the fit parameters (other than line mixing coefficients) were taken from HITRAN 2004 database [15] (the line positions for the transition in our bands are the same as in the recent HITRAN 2008 database [16]). During the analysis the line parameters for unmeasured lines were fixed to values reported in the HITRAN database [15]. For these unmeasured lines we kept the temperature dependences of their shift coefficients set to zero, an assumption that did not seem to affect the quality of the fits as judged from the fit residuals.

The low pressure spectra were used to determine an internal calibration factor with reference to the positions of select carbon dioxide transitions, as reported in HITRAN 2004 [15]. The calibration factors obtained by this method were then used to calibrate spectra recorded in the same day and at elevated temperatures.

Below we present the expressions used to retrieve the self-broadened half width and pressure induced shift coefficients and their temperature dependences:

$$\gamma(p,T) = p\gamma^0(p_0,T_0)\left[\frac{T_0}{T}\right]^n \quad (1)$$

$$v = v_0 + p\delta^0 \quad (2)$$

$$\delta^0(T) = \delta^0(T_0) + \delta'(T - T_0) \quad (3)$$

In Eqs. (1)–(3) the reference pressure and temperature are p_0=1 atm and T_0=296 K, respectively. γ^0 is the retrieved self-broadened half-width coefficient at the reference pressure p_0 (1 atm) and reference temperature T_0 (296 K). γ is the measured self-broadened half width coefficient of the spectral line and p is the total sample pressure. n is the temperature dependence exponent of the self-broadened half-width coefficient. δ^0 is the pressure-induced shift coefficient, v is the measured line position, v_0 is the position at zero pressure, and δ' is the temperature dependent coefficient of the self-induced pressure shift coefficients.

Based on the conclusions of the room temperature spectroscopic studies of the 30013←00001 and 30012←00001 bands [2–4], we have accounted for line mixing effects in our line shape modeling. At elevated pressures inelastic collisions redistribute the molecules between adjacent energy levels, leading to a transfer of intensity from some parts of the spectrum to others. As a consequence, in the weak line mixing regime, the spectral lines are asymmetric. The line asymmetry is modeled in our analysis software by adding a dispersive profile of amplitude $pY_{0k}(T)$ to the non-dispersive Voigt or speed-dependent Voigt profiles [Eq. (4)], where p is the gas pressure in atm and $Y_{0k}(T)$ is the line mixing coefficient of the transition of interest.

As in our previous studies [4,17] we have described the state of the molecules using the relaxation matrix formalism, where the self-broadening coefficients are the real parts of the diagonal elements of the relaxation matrix, W, and the pressure-induced line shift coefficients are the imaginary parts of the diagonal elements. The weak self-line mixing coefficients, Y_{0k} at a given temperature T, are quantified using the off-diagonal elements of the W matrix:

$$Y_{0k}(T) = 2\sum_{j\neq k}\frac{d_j}{d_k}\frac{W_{jk}}{v_k - v_j} \quad (4)$$

The line mixing coefficients $Y_{0k}(T)$ calculated in this way account for collisional transfer between pairs of energy levels j and k. In Eq. (4), d_k are the elements of the dipole moment matrix.

The resulting line parameters determined from multispectrum least squares fits are listed in Tables 2 and 3 for the 30013←00001 and 30012←00001 bands, respectively. We were unable to retrieve experimentally

Table 2
Temperature dependences of self-broadened half width and pressure shift coefficients in the 30013←00001 band of carbon dioxide.

m	Position (cm^{-1})[a]	n		δ' ($cm^{-1}\,atm^{-1}\,K^{-1}$)	
		VOIGT	SDV	VOIGT	SDV
−56	6173.169436	0.539(7)	0.522(7)		
−54	6175.528804	0.523(7)	0.508(7)		
−52	6177.856588	0.533(7)	0.563(7)		
−50	6180.152998	0.536(7)	0.600(8)		
−48	6182.418249	0.515(7)	0.564(7)		
−46	6184.652553	0.429(6)	0.517(7)	0.000068(3)	0.000037(3)
−44	6186.856124	0.502(7)	0.524(7)	0.000088(4)	0.000106(4)
−42	6189.029173	0.526(7)	0.566(7)	0.000067(3)	0.000073(2)
−40	6191.171908	0.579(8)	0.589(8)	0.000053(2)	0.000066(2)
−38	6193.284533	0.585(11)	0.584(11)	0.000074(3)	0.000072(3)
−36	6195.367248	0.616(9)	0.639(9)	0.000059(2)	0.000054(3)
−34	6197.420244	0.568(8)	0.583(8)	0.000088(3)	0.000076(4)
−32	6199.443709	0.602(7)	0.623(7)	0.000090(3)	0.000079(4)
−30	6201.437820	0.666(6)	0.679(6)	0.000091(5)	0.000082(3)
−28	6203.402748	0.664(6)	0.681(6)	0.000103(3)	0.000088(5)
−26	6205.338653	0.637(6)	0.638(6)	0.000098(3)	0.000080(5)
−24	6207.245685	0.669(5)	0.676(5)	0.000131(4)	0.000099(7)
−22	6209.123984	0.679(5)	0.689(5)	0.000086(3)	0.000076(3)
−20	6210.973679	0.722(5)	0.722(5)	0.000056(2)	0.000038(3)
−18	6212.794885	0.704(5)	0.703(5)	0.000081(2)	0.000062(2)
−16	6214.587708	0.701(4)	0.676(4)	0.000097(5)	0.000090(5)
−14	6216.352238	0.734(4)	0.729(4)	0.000065(2)	0.000034(3)
−12	6218.088553	0.704(5)	0.704(5)	0.000079(4)	0.000067(4)
−10	6219.796718	0.759(4)	0.762(4)	0.000151(6)	0.000142(5)
−8	6221.476784	0.823(4)	0.821(4)	0.000101(4)	0.000083(5)
−6	6223.128787	0.772(4)	0.782(4)	0.000033(1)	0.000001(1)
−4	6224.752748	0.699(5)	0.705(5)	0.000039(2)	0.000016(1)
−2	6226.348676	0.760(5)	0.718(5)	0.000100(5)	0.000060(4)
1	6228.689985	0.814(5)	0.794(5)	0.000072(3)	0.000106(3)
3	6230.215765	0.744(6)	0.776(6)	0.000065(3)	0.000062(3)
5	6231.713422	0.702(8)	0.737(8)	0.000058(2)	0.000086(2)
7	6233.182896	0.638(5)	0.677(5)	0.000081(4)	0.000096(4)
9	6234.624116	0.636(5)	0.664(5)	0.000078(3)	0.000085(3)
11	6236.036992	0.648(5)	0.654(5)	0.000105(3)	0.000109(4)
13	6237.421424	0.693(4)	0.716(4)	0.000092(4)	0.000065(5)
15	6238.777296	0.688(4)	0.705(4)	0.000090(3)	0.000080(4)
17	6240.104478	0.675(4)	0.670(4)	0.000068(3)	0.000023(2)
19	6241.402828	0.629(4)	0.631(4)	0.000051(3)	0.000077(3)
21	6242.672191	0.630(4)	0.635(4)	0.000129(6)	0.000154(6)
23	6243.912398	0.643(4)	0.669(4)	0.000121(4)	0.000140(4)
25	6245.123271	0.615(5)	0.640(5)	0.000087(3)	0.000102(3)
27	6246.304618	0.615(5)	0.627(5)	0.000106(5)	0.000111(4)
29	6247.456239	0.659(5)	0.652(5)	0.000053(2)	0.000066(2)
31	6248.577920	0.622(5)	0.621(5)	0.000067(2)	0.000095(3)
33	6249.669442	0.650(6)	0.613(6)	0.000111(4)	0.000135(4)
35	6250.730575	0.663(6)	0.641(6)	0.000119(5)	0.000146(6)
37	6251.761081	0.527(6)	0.528(6)	0.000132(7)	0.000140(7)
39	6252.760717	0.635(7)	0.614(7)	0.000088(3)	0.000091(3)
41	6253.729232	0.625(8)	0.602(8)	0.000045(2)	0.000093(2)
43	6254.666372	0.545(8)	0.541(8)	0.000070(3)	0.000077(2)
45	6255.571877	0.587(8)	0.591(8)	0.000092(4)	0.000154(5)
47	6256.445485	0.609(8)	0.663(9)	0.000097(5)	0.000200(3)
49	6257.286932	0.600(8)	0.590(8)	0.000040(1)	0.000138(2)
51	6258.095953	0.540(7)	0.542(7)	0.000044(2)	0.000048(2)
53	6258.872284	0.539(7)	0.599(8)		
55	6259.615664	0.607(8)	0.605(8)		

[a] Line positions are taken from HITRAN2008 [16].

Table 3
Temperature dependences of self-broadened half width and pressure shift coefficients in the 30012←00001 band of carbon dioxide.

m	Position (cm^{-1})[a]	n		δ' ($cm^{-1}\,atm^{-1}\,K^{-1}$)	
		VOIGT	SDV	VOIGT	SDV
−56	6292.996793	0.501(7)	0.552(7)		
−54	6295.319763	0.428(6)	0.441(6)		
−52	6297.618698	0.603(8)	0.630(8)		
−50	6299.893141	0.635(8)	0.651(8)		
−48	6302.142653	0.575(7)	0.588(8)		
−46	6304.366820	0.595(8)	0.614(8)	0.000054(3)	0.000061(2)
−44	6306.565247	0.518(7)	0.522(7)	0.000109(4)	0.000105(5)
−42	6308.737560	0.524(7)	0.532(7)	0.000054(2)	0.000073(2)
−40	6310.883410	0.526(7)	0.530(7)	0.000074(2)	0.000061(3)
−38	6313.002450	0.555(11)	0.555(11)	0.000058(2)	0.000063(2)
−36	6315.094370	0.537(9)	0.548(9)	0.000040(2)	0.000045(2)
−34	6317.158870	0.562(8)	0.575(8)	0.000055(3)	0.000056(3)
−32	6319.195680	0.515(7)	0.531(7)	0.000060(2)	0.000064(2)
−30	6321.204520	0.624(6)	0.635(6)	0.000076(4)	0.000073(2)
−28	6323.185160	0.625(6)	0.634(6)	0.000068(3)	0.000076(3)
−26	6325.137350	0.608(6)	0.620(6)	0.000059(2)	0.000066(2)
−24	6327.060900	0.603(5)	0.620(5)	0.000086(4)	0.000102(4)
−22	6328.955590	0.622(5)	0.636(5)	0.000067(3)	0.000066(2)
−20	6330.821240	0.640(5)	0.648(5)	0.000021(1)	0.000031(1)
−18	6332.657690	0.684(5)	0.690(5)	0.000045(1)	0.000035(1)
−16	6334.464790	0.627(4)	0.636(4)	0.000070(2)	0.000059(2)
−14	6336.242380	0.666(4)	0.675(4)	0.000055(2)	0.000012(3)
−12	6337.990360	0.745(5)	0.744(5)	0.000031(2)	0.000042(2)
−10	6339.708600	0.709(4)	0.718(4)	0.000116(5)	0.000093(3)
−8	6341.397010	0.816(4)	0.803(4)	0.000062(2)	0.000078(3)
−6	6343.055515	0.701(4)	0.711(4)	0.000017(1)	0.000011(1)
−4	6344.684033	0.633(5)	0.654(5)	0.000039(2)	0.000019(2)
−2	6346.282512	0.687(5)	0.702(5)	0.000086(4)	0.000087(3)
1	6348.623821	0.719(5)	0.732(5)	0.000096(4)	0.000081(5)
3	6350.147049	0.871(6)	0.871(6)	0.000030(1)	0.000039(1)
5	6351.640150	0.676(8)	0.692(8)	0.000076(2)	0.000047(4)
7	6353.103127	0.704(5)	0.715(5)	0.000068(3)	0.000062(3)
9	6354.535999	0.650(5)	0.657(5)	0.000063(3)	0.000047(3)
11	6355.938798	0.686(5)	0.688(5)	0.000067(3)	0.000055(3)
13	6357.311571	0.571(4)	0.588(4)	0.000078(2)	0.000010(3)
15	6358.654375	0.736(4)	0.740(4)	0.000043(2)	0.000065(2)
17	6359.967287	0.660(4)	0.669(4)	0.000063(3)	0.000031(3)
19	6361.250392	0.638(4)	0.645(4)	0.000074(2)	0.000051(2)
21	6362.503794	0.684(4)	0.694(4)	0.000134(7)	0.000103(5)
23	6363.727610	0.646(4)	0.654(4)	0.000123(4)	0.000107(5)
25	6364.921972	0.693(5)	0.699(5)	0.000085(4)	0.000074(3)
27	6366.087029	0.647(5)	0.644(5)	0.000073(4)	0.000068(2)
29	6367.222942	0.640(5)	0.645(5)	0.000053(2)	0.000039(2)
31	6368.329891	0.688(5)	0.689(5)	0.000093(5)	0.000058(4)
33	6369.408072	0.650(6)	0.652(6)	0.000113(3)	0.000095(5)
35	6370.457697	0.587(6)	0.592(6)	0.000137(7)	0.000109(5)
37	6371.478995	0.545(6)	0.538(6)	0.000097(3)	0.000104(5)
39	6372.472214	0.519(7)	0.531(7)	0.000064(3)	0.000057(3)
41	6373.437620	0.563(8)	0.567(8)	0.000106(3)	0.000060(4)
43	6374.375495	0.515(8)	0.525(8)	0.000055(2)	0.000054(3)
45	6375.286144	0.552(7)	0.564(7)	0.000101(3)	0.000067(3)
47	6376.169890	0.496(6)	0.516(7)	0.000096(3)	0.000109(4)
49	6377.027075	0.567(7)	0.547(7)	0.000069(3)	0.000113(3)
51	6377.858065	0.59(8)	0.558(7)	0.000064(3)	0.000129(3)
53	6378.663244	0.597(8)	0.559(7)		
55	6379.443023	0.614(8)	0.652(8)		

[a] Line positions are from HITRAN2008 [16].

the line mixing coefficients for the spectra recorded at the lowest temperature. But, for consistency in the multi-spectrum fits at 217 K, we have modeled the spectral profiles using calculated line mixing coefficients obtained using the Exponential Power Gap law and our parameters from Ref. [17]. The line positions taken from HITRAN 2008 [16] are shown for easy identification of the transitions.

3. Theoretical calculations

The real components of the semiclassical Robert–Bonamy formalism [13], (RRB), was used to calculate the self-broadened half-widths of carbon dioxide. In computational form, the half-width γ of any given rovibrational transition $f \leftarrow i$ is expressed in terms of the elements of the Liouville scattering matrix [18,19]:

$$\lambda_{f\leftarrow i} = \frac{n_2}{2\pi c} \langle v[1-e^{-S_2(f,i,J_2,v,b)}] \rangle_{v,b,J_2} \quad (5)$$

In Eq. (5) n_2 is the number density of perturbers and $\langle\ \rangle_{v,b,J_2}$ is an average over all possible molecular trajectories of impact parameter b, initial relative velocity v, and the initial rotational quantum number J_2 of the collision partner. The physical meaning of the S_2 term was

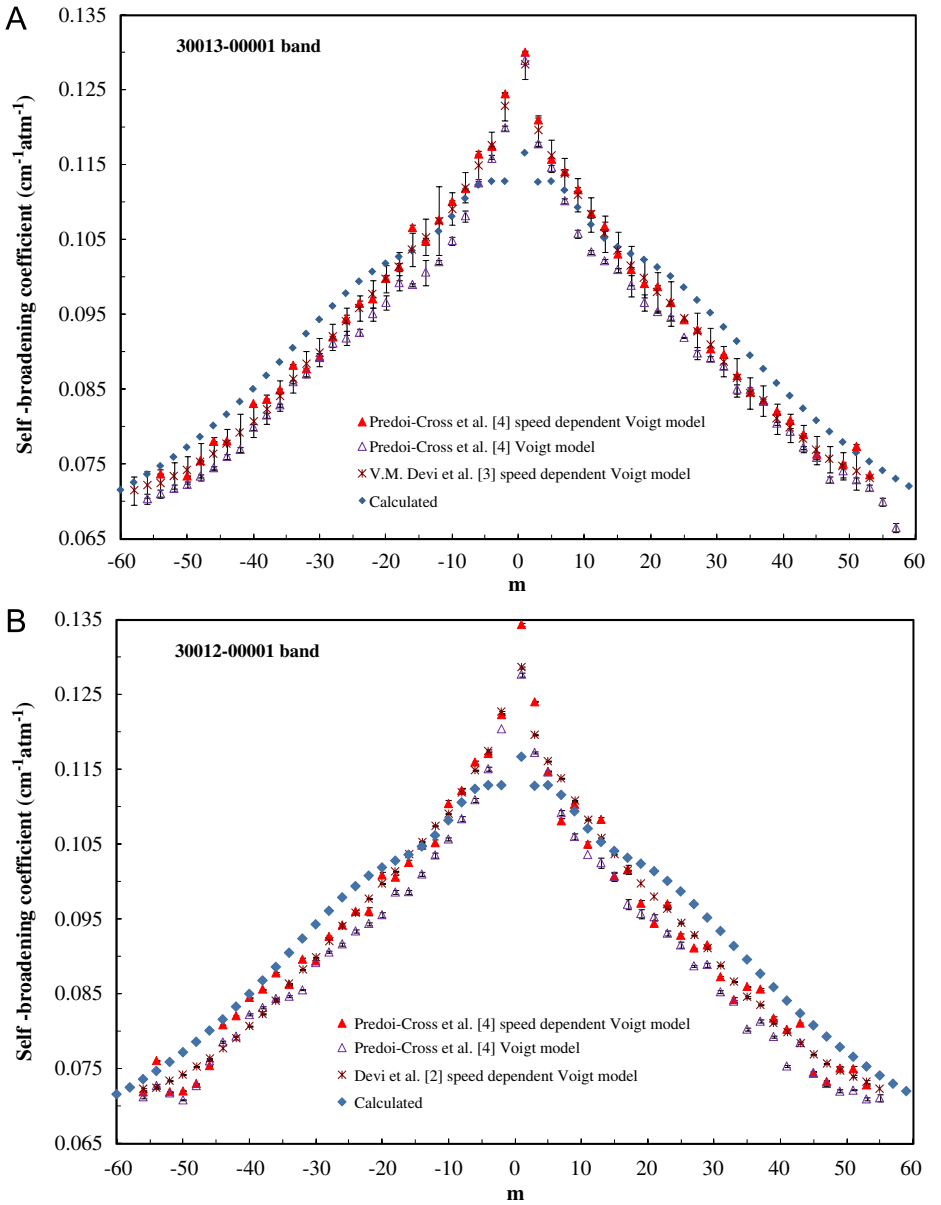

Fig. 1. Experimental room temperature self-broadening coefficients for the 30013←00001 (panel A) and 30012←00001 (panel B) bands of $^{12}C^{16}O_2$ retrieved using multispectrum fits [14]. We present both results obtained with the Voigt and speed dependent Voigt models. The calculated self-broadening coefficients are overlaid to our results.

discussed in Ref. [13]. For the convenience of the reader, we will discuss them here as well. $Re(S_2)$ is the real part of the second order term in the successive expansion of the corresponding scattering matrix and depends on (i) the rovibrational states involved in the transition and associated collision induced jumps from these energy levels, (ii) the intermolecular potential, and (iii) the collision dynamics.

The intermolecular potential was modeled using the electrostatic (quadrupole–quadrupole) component of the CO_2–CO_2 system and an atom–atom interaction to account for close collisions. The expression of Sack [20] expanded to the fourth order was used to express the atom–atom distance, r_{ij}, in terms of the center of mass separation, R. Robert and Bonamy's second order in time approximation [13] is used to describe the dynamics of the collisional processes. In this approximation the interaction potential is used to determine the distance, effective velocity, and force at closest approach. To simplify the trajectory calculations the isotropic part of the atom–atom expansion is approximated by a single isotropic Lennard-Jones 6–12 potential where the molecular parameters are from Ref. [21]. The reduced matrix elements of the radiating and perturbing molecules are evaluated using wavefunctions in the symmetric top basis and the energies are given in terms of the molecular rotational constants [22].

There are a number of different methods that have been proposed to determine heteronuclear potential atom–atom parameters from the homonuclear parameters [23 (and references therein), 24]. Good and Hope [25] showed that different combination rules to determine ε show variations of ~15%. Depending on how the values are derived it is possible to find examples in the literature [26] where the parameters for the same interaction pair differ by factors of 2.

There are several studies that show when the molecular parameters are adjusted, the resulting half-widths agree better with experiment [21,27–29]. Thus it appears reasonable to adjust the molecular parameters when measurements are available.

Here, initial calculations for the transitions studied in the 30012←00001 band were made at 296 K using the molecular parameters taken from the work of Rosenmann et al. [21]. The calculations show an average difference of 7.3% compared with the measurements. Next, each atom–atom coefficient (D0, E0, DO, EO) and the quadruple moment was changed, one at a time, by 10% and the calculations made to determine the dependence of the half-widths on these parameters. With this information the parameters were adjusted iteratively and the calculations compared with the measurements until we achieved a percent difference of just under 2.

The final values of the parameters are a 10% reduction in the quadrupole moment, 15% increase in the D0 and EO atom–atom parameters and a 15% decrease in the E0 and DO atom–atom parameters.

The calculations of self-broadened half-width coefficients were made for P- and R-branch transitions of CO_2 for $|m|$ values from 1 to 64. The half-width coefficients were calculated at 200, 250, 296, 350, and

Table 4
Half-widths at 296 K and temperature dependence of the half-width calculated using Eq. (5).

J'	J''	30012←00001 band		30013←00001 band	
		γ	n	J'	J''
1	2	0.1129	0.74(.01)	0.1129	0.74(.01)
3	4	0.1129	0.74(.00)	0.1129	0.74(.00)
5	6	0.1124	0.72(.01)	0.1124	0.72(.01)
7	8	0.1106	0.69(.01)	0.1106	0.69(.01)
9	10	0.1082	0.68(.01)	0.1082	0.68(.01)
11	12	0.1062	0.69(.03)	0.1062	0.69(.03)
13	14	0.1047	0.70(.03)	0.1047	0.70(.03)
15	16	0.1036	0.71(.02)	0.1036	0.71(.02)
17	18	0.1028	0.71(.01)	0.1028	0.71(.01)
19	20	0.1019	0.70(.01)	0.1019	0.70(.01)
21	22	0.1008	0.69(.02)	0.1008	0.69(.02)
23	24	0.0994	0.68(.02)	0.0995	0.68(.02)
25	26	0.0979	0.66(.02)	0.0979	0.66(.02)
27	28	0.0961	0.65(.01)	0.0962	0.65(.01)
29	30	0.0943	0.63(.01)	0.0944	0.63(.01)
31	32	0.0924	0.62(.02)	0.0925	0.62(.02)
33	34	0.0905	0.61(.02)	0.0906	0.61(.02)
35	36	0.0886	0.61(.04)	0.0887	0.61(.04)
37	38	0.0868	0.60(.05)	0.0869	0.60(.05)
39	40	0.0850	0.59(.06)	0.0851	0.59(.06)
41	42	0.0833	0.59(.08)	0.0834	0.59(.07)
43	44	0.0816	0.59(.09)	0.0817	0.59(.09)
45	46	0.0801	0.59(.10)	0.0802	0.59(.10)
47	48	0.0786	0.59(.11)	0.0787	0.59(.11)
49	50	0.0772	0.59(.12)	0.0773	0.59(.12)
51	52	0.0759	0.60(.13)	0.0760	0.60(.13)
53	54	0.0747	0.60(.13)	0.0748	0.60(.13)
55	56	0.0736	0.60(.14)	0.0737	0.60(.14)
57	58	0.0725	0.61(.14)	0.0726	0.61(.14)
59	60	0.0716	0.61(.14)	0.0716	0.61(.14)
61	62	0.0706	0.62(.14)	0.0707	0.62(.14)
63	64	0.0698	0.62(.13)	0.0698	0.62(.13)
1	0	0.1167	0.73(.01)	0.1167	0.73(.01)
3	2	0.1128	0.74(.00)	0.1128	0.74(.00)
5	4	0.1129	0.73(.01)	0.1129	0.73(.01)
7	6	0.1116	0.70(.01)	0.1117	0.70(.01)
9	8	0.1094	0.69(.00)	0.1094	0.69(.00)
11	10	0.1071	0.68(.02)	0.1071	0.68(.02)
13	12	0.1053	0.69(.03)	0.1053	0.69(.03)
15	14	0.1041	0.70(.02)	0.1041	0.70(.02)
17	16	0.1032	0.71(.02)	0.1032	0.71(.02)
19	18	0.1024	0.71(.01)	0.1024	0.71(.01)
21	20	0.1014	0.70(.02)	0.1014	0.70(.02)
23	22	0.1001	0.69(.02)	0.1002	0.69(.02)
25	24	0.0987	0.67(.02)	0.0987	0.67(.02)
27	26	0.0970	0.65(.02)	0.0970	0.65(.02)
29	28	0.0952	0.64(.01)	0.0953	0.64(.01)
31	30	0.0934	0.63(.01)	0.0934	0.63(.01)
33	32	0.0914	0.62(.02)	0.0915	0.62(.02)
35	34	0.0896	0.61(.03)	0.0896	0.61(.03)
37	36	0.0877	0.60(.04)	0.0878	0.60(.04)
39	38	0.0859	0.60(.06)	0.0859	0.60(.06)
41	40	0.0841	0.59(.07)	0.0842	0.59(.07)
43	42	0.0824	0.59(.08)	0.0825	0.59(.08)
45	44	0.0808	0.59(.09)	0.0809	0.59(.09)
47	46	0.0793	0.59(.10)	0.0794	0.59(.10)
49	48	0.0779	0.59(.11)	0.0780	0.59(.11)
51	50	0.0766	0.59(.12)	0.0766	0.59(.12)
53	52	0.0753	0.60(.13)	0.0754	0.60(.13)
55	54	0.0741	0.60(.14)	0.0742	0.60(.14)
57	56	0.0730	0.61(.14)	0.0731	0.61(.14)
59	58	0.0720	0.61(.14)	0.0721	0.61(.14)
61	60	0.0711	0.62(.14)	0.0712	0.61(.14)
63	62	0.0702	0.62(.14)	0.0703	0.62(.14)
65	64	0.0693	0.62(.13)	0.0694	0.62(.13)

The calculated values are plotted in Figs. 1A and B.

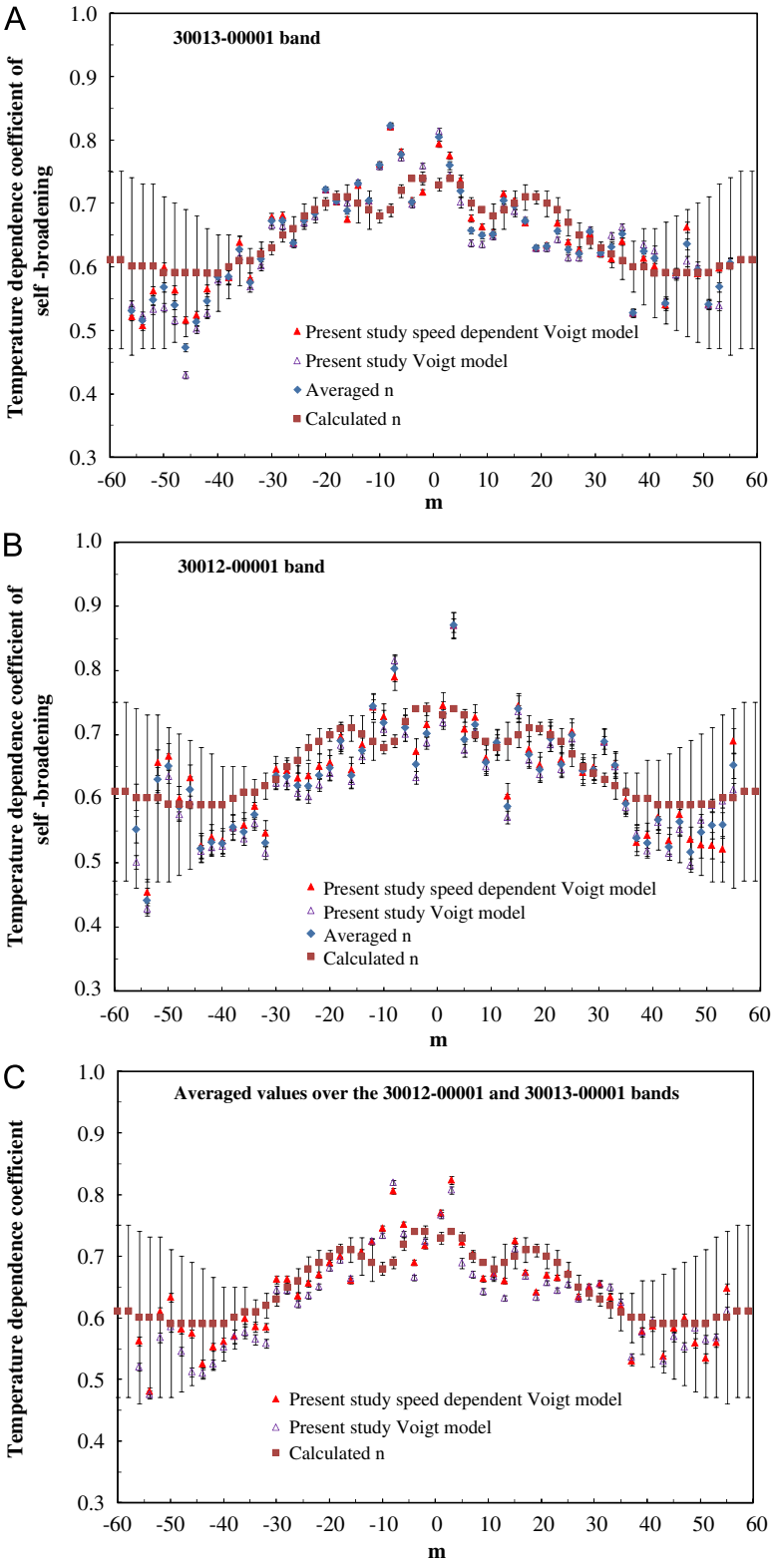

Fig. 2. Experimental and calculated temperature dependence exponents of self-broadening coefficients for the 30013←00001 (panel A) and 30012←00001 (panel B) bands of CO_2. We plot our results obtained with the Voigt and with the speed dependent Voigt models. The experimental and calculated results obtained for the two bands are presented in panel C.

500 K via Eq. (5). In Figs. 1A and B the calculations are compared with measurements for the 30013-00001 and 30012-00001 bands. We have plotted the self-broadening coefficients for the 30013←00001 (panel A) and 30012←00001 (panel B) bands as a function of m (where $m=-J''$ for P branch lines and $J''+1$ for R branch lines). The error bars for the experimental results are also plotted.

For atmospheric applications, both the temperature and pressure dependence of half-width coefficients are required on a line-by-line basis. The temperature scaling law [30] and Eq. (1). can be used to determine the temperature dependence exponents, n, of the self-broadened half-width coefficients.

In recent years it has been shown that for some gas-perturber systems, such as for example, foreign-gas broadened water, this scaling law is not always appropriate [31–34]. It will be shown below that the power-law model does not work reasonably well for the CO_2–CO_2 system.

The theoretical values of the temperature dependence exponents, n, were determined for each transition by a least-squares fits of $\ln[\gamma(T)/\gamma(T_0)]$ vs. $\ln[T_0/T]$ over the temperature range 200–500 K. We estimate the error in the temperature dependence exponents using the half-width values at any two of the five temperatures studied. This procedure provided ten 2-point temperature dependence exponents. The difference between each 2-point

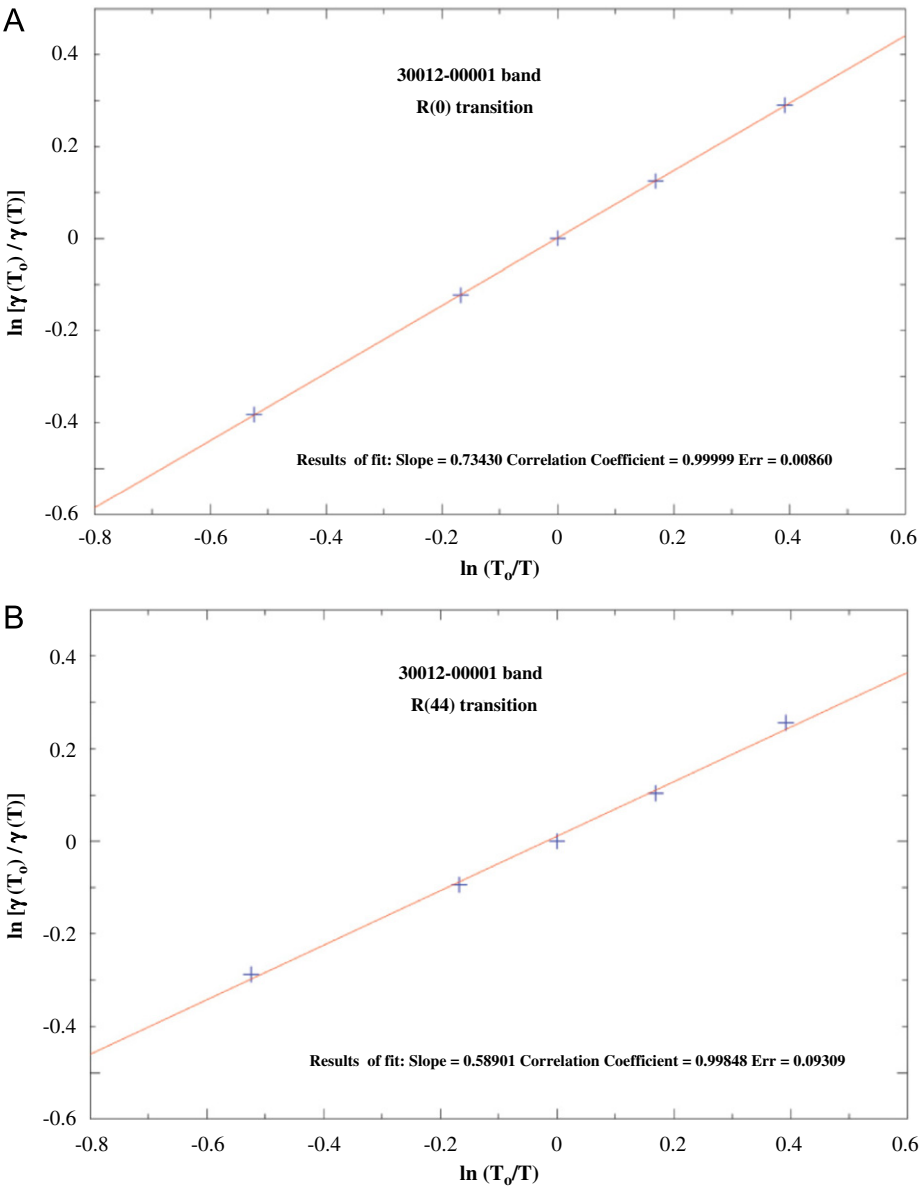

Fig. 3. Fits of $\ln[\gamma(T_0)/\gamma(T)]$ as a function of $\ln(T_0/T)$ for the $R(0)$ (panel A) and $R(44)$ (panel B) transitions of the 30012←00001 band using self-broadened widths calculated over the range 200–500 K.

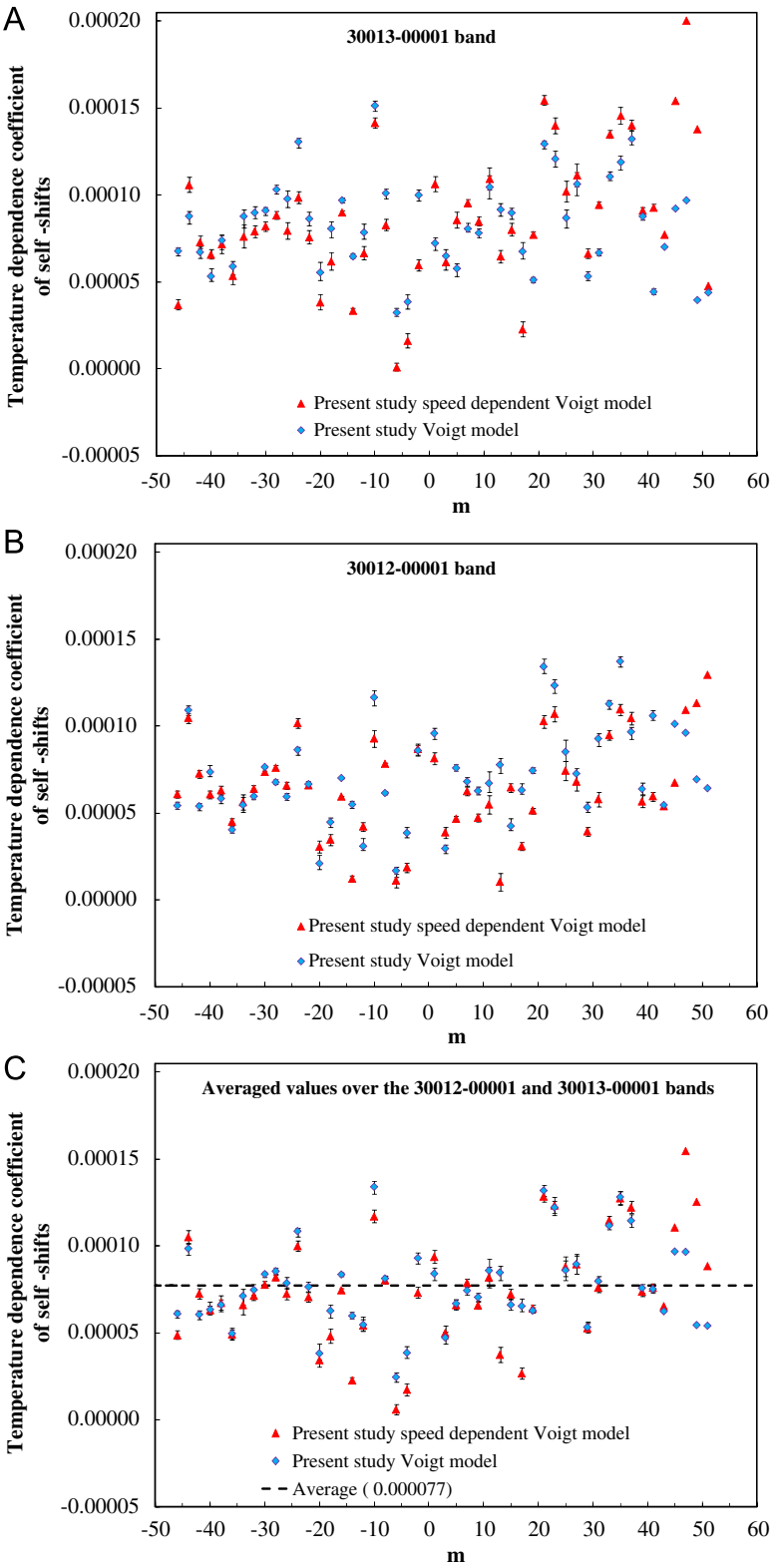

Fig. 4. Measured temperature dependence exponents of self-pressure shift coefficients for the 30013←00001 (panel A) and 30012←00001 (panel B) bands of CO_2. Plotted are results retrieved with the Voigt and with the speed dependent Voigt models. The results obtained for the two bands are averaged and plotted in panel C.

temperature dependence exponent and the 5-point fit value is calculated. The errors quoted in this work are the largest of these differences and believed to be more reliable than the statistical values taken from the fit.

4. Comparison of experiment and calculations

The calculated widths and their temperature dependences are given in Table 4. These data are compared with the present measurements plotted in Figs. 1A and B. The agreement is quite good as seen in the figures. In both bands, for $|m|$ above 3 the observed self-broadening coefficients for both the P and R branch transitions lie on a smoothly changing curve, below the calculated values.

In Figs. 2A and B we have plotted the temperature dependence exponents of the self-broadening coefficients, n, as a function of m for the 30013←00001 (panel A) and 30012←00001 (panel B) bands. Similar to our observations for the temperature dependence exponents of the air-broadened widths [12], the measured n vs. m show much scatter. For the same m values, small variations are observed when we change the line shape model from Voigt to speed-dependent Voigt. Also, as pointed out in Ref. [12], comparing the values for n in the two bands (panels A and B), for the same line shape model and the same m value, we observed that the differences are small. In panel C we have plotted the averaged experimental and calculated values for the same m values and transitions in the two bands.

In all three panels of Fig. 2 the reader can note that there is good agreement between the experimental values for temperature dependences of self-broadening coefficients, n, and the calculated ones. Clearly, the pattern in the calculated n values with a local minimum at $|m|$ equal to -10 and 9, is not reproduced in the experimental results. We believe that there is need of more measurements for temperature dependence of self-broadening coefficients at both higher and lower temperatures than the limited range covered in this study. Extending the temperature range will greatly reduce the uncertainty of the derived n value as shown by Gamache et al. [35]. In our study the transitions were fairly weak above $|m|=40$ and we believe that in order to validate the calculations at high J values, new studies for stronger bands are needed.

The accuracy of the power law model of the temperature dependence applied to the half-width for the CO_2–CO_2 system varies as a function of the J''. In Figs. 3A and B are the fits for the $R(0)$ and $R(44)$ transitions of the 30012←00001 band calculated over the range 200–500 K. The fit for the low J'' transition ($J''=0$) (see Fig. 3A) is good

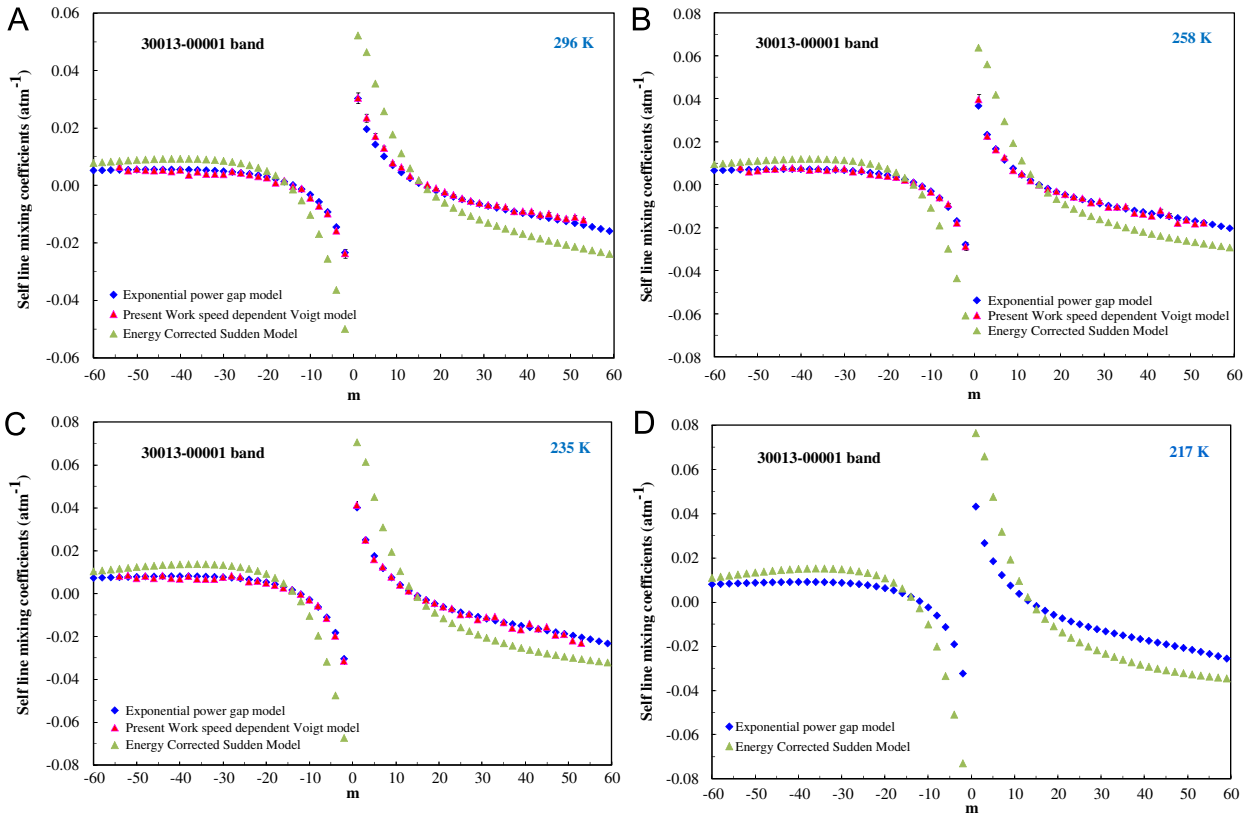

Fig. 5. Overlaid measured and calculated [17] line mixing parameters using the Exponential Power Gap Law (EPG) and Energy Corrected Sudden (ECS) law, respectively. The results are plotted against m for transitions in the 30013←00001 band at 296 K (panel A), 258 K (panel B), 235 K (panel C) and 217 K (panel D).

as seen in the correlation coefficient of the fit, R=0.99999. Inspection of the curve finds most of the points on or near the straight line. However, as J'' increases the points are no longer in a straight line as seen in Fig. 3B where the correlation coefficient reaches 0.99848.

The measured temperature dependence coefficients of the self-pressure induced shifts, δ', are plotted in Fig. 4 as a function of m for the 30013←00001 (panel A) and 30012←00001 (panel B) bands. The parameter errors are less than 6% for both the values fitted with the Voigt and speed dependent Voigt profiles. The scatter in our temperature dependence coefficients of the self-pressure induced shifts occurs mostly at high $|m|$ values or in spectral regions where the measured transitions overlap with hot band transitions. In panel C we have plotted the averaged values for δ' for the two sets of results along with the average over the two bands ($0.000077\,cm^{-1}\,atm^{-1}\,K^{-1}$). A very interesting finding is that the average values are close in absolute value of the mean temperature dependence of the air-broadened shift coefficients ($-0.00006\,cm^{-1}\,atm^{-1}\,K^{-1}$) [12] but of opposite sign!

In Figs. 5 and 6 we have compared our experimental line mixing results for the sets of spectra recorded at room temperature [4], 258 and 235 K with values calculated using the Exponential Power Gap (EPG) scaling law and the Energy Corrected Sudden (ECS) model and our parameters for temperature dependence reported in Ref. [17]. The measured and calculated results are plotted against m. The results obtained for transitions in the 30013←00001 band are shown in Fig. 5 and those for the 30012←00001 band in Fig. 6. In both figures the top panel presents our room temperature results from Ref. [17]. Since, as mentioned in previous sections, we were unable to retrieve the experimental self-line mixing coefficients at 217 K, in panels D of Figs. 5 and 6, we have plotted the calculated line mixing coefficients expected at this temperature.

As shown in Ref. [17], the adjustable parameters from the scaling laws have a temperature dependence that has to be taken into account to ensure a good agreement between the experimental values of broadening coefficients and those calculated using scaling laws over a wide temperature range.

In the case of modeling the line mixing coefficients with the EPG scaling law, the temperature dependence coefficients (see Eq. (8) of Ref. [17]) of the parameter used to describe the collisional rates in Eq. (5) of Ref. [17] were taken from Table 3A of Ref. [17]. The room temperature values for the adjustable EPG parameters for self-broadened transitions in the 30013←00001 and the 30012←00001 bands, were taken

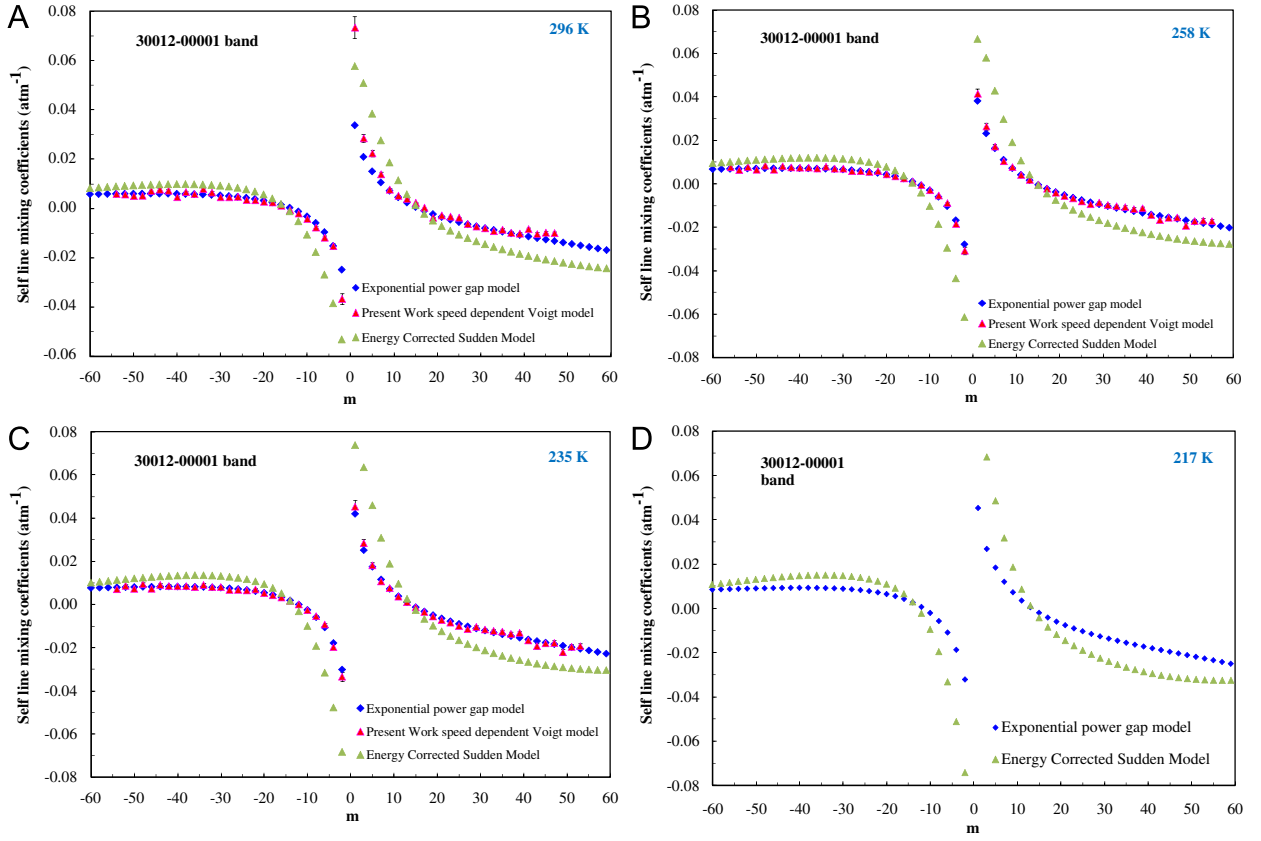

Fig. 6. Overlaid measured and calculated [17] line mixing results parameters using the Exponential Power Gap Law (EPG) and Energy Corrected Sudden (ECS) law, respectively. The results are plotted against m for transitions in the 30012←00001 band at 296 K (panel A), 258 K (panel B), 235 K (panel C) and 217 K (panel D).

from Table 1 of Ref. [17]. As can be seen in panels A–C of Figs. 5 and 6 the EPG law reproduces the observed self-line mixing coefficients to within ±10% of the experimental values. In Figs. 5 and 6 the self-line mixing coefficients retrieved at 296, 258 and 235 K and the calculated ones for 217 K are given in Tables 5 and 6 for the 30013←00001 and the 30012←00001 bands, respectively.

Table 5
Self line mixing coefficients in the 30013←00001 band of carbon dioxide.

m	Position (cm^{-1})[a]	Y (296 K) (atm^{-1}) [4]	Y (258 K) (atm^{-1})		Y (235 K) (atm^{-1})		Y (217 K) (atm^{-1})	
		SDV	VOIGT	SDV	VOIGT	SDV	EPG	ECS
−56	6173.169436						0.0084	0.0120
−54	6175.528804	0.0064(5)	0.0079(5)	0.0083(7)	0.0083(5)	0.0086(7)	0.0085	0.0125
−52	6177.856588	0.0051(4)	0.006(3)	0.0063(6)	0.0087(3)	0.0091(6)	0.0087	0.0129
−50	6180.152998	0.0056(4)	0.0065(8)	0.0065(7)	0.0073(8)	0.0073(7)	0.0088	0.0134
−48	6182.418249	0.0052(4)	0.0072(8)	0.0073(5)	0.0083(8)	0.0085(5)	0.0089	0.0138
−46	6184.652553	0.0051(4)	0.0073(3)	0.0074(9)	0.0073(3)	0.0074(9)	0.0090	0.0142
−44	6186.856124	0.0053(3)	0.0081(5)	0.0075(9)	0.0085(5)	0.0079(9)	0.0091	0.0145
−42	6189.029173	0.0048(3)	0.0077(7)	0.0070(3)	0.0073(7)	0.0066(3)	0.0091	0.0148
−40	6191.171908	0.0054(3)	0.0076(4)	0.0075(4)	0.0070(4)	0.0069(4)	0.0092	0.0150
−38	6193.284533	0.0036(5)	0.0067(3)	0.0067(6)	0.0083(3)	0.0082(6)	0.0092	0.0152
−36	6195.367248	0.0047(5)	0.0073(8)	0.0070(4)	0.0070(8)	0.0067(4)	0.0092	0.0152
−34	6197.420244	0.0039(4)	0.0067(2)	0.0073(3)	0.0069(2)	0.0076(3)	0.0091	0.0152
−32	6199.443709	0.0039(4)	0.0075(8)	0.0068(3)	0.0069(8)	0.0063(3)	0.0090	0.0151
−30	6201.437820	0.0038(4)	0.0074(2)	0.0069(6)	0.0078(2)	0.0073(6)	0.0088	0.0148
−28	6203.402748	0.0048(4)	0.0060(4)	0.0056(3)	0.0085(4)	0.0079(3)	0.0085	0.0145
−26	6205.338653	0.0043(5)	0.0068(8)	0.0072(3)	0.0080(8)	0.0085(3)	0.0082	0.0139
−24	6207.245685	0.0037(5)	0.0048(2)	0.0046(4)	0.0057(2)	0.0055(4)	0.0077	0.0132
−22	6209.123984	0.0031(3)	0.0044(4)	0.0045(3)	0.0060(4)	0.0062(3)	0.0071	0.0122
−20	6210.973679	0.0027(1)	0.0039(6)	0.0035(4)	0.0052(6)	0.0046(4)	0.0064	0.0108
−18	6212.794885	0.0009(1)	0.0034(7)	0.0031(4)	0.0040(7)	0.0037(4)	0.0054	0.0088
−16	6214.587708	0.0016(1)	0.0022(4)	0.0023(3)	0.0029(4)	0.0031(3)	0.0041	0.0062
−14	6216.352238	−0.0003(1)	0.0011(3)	0.0011(4)	0.0019(3)	0.0019(4)	0.0025	0.0024
−12	6218.088553	−0.0011(1)	−0.0008(2)	−0.0008(3)	−0.0001(2)	−0.0001(3)	0.0004	−0.0028
−10	6219.796718	−0.0043(5)	−0.0034(6)	−0.0035(4)	−0.0027(6)	−0.0028(4)	−0.0023	−0.0101
−8	6221.476784	−0.0071(6)	−0.0060(7)	−0.0055(3)	−0.0055(7)	−0.0051(3)	−0.0061	−0.0201
−6	6223.128787	−0.0098(6)	−0.0091(3)	−0.0082(4)	−0.0113(3)	−0.0102(4)	−0.0113	−0.0334
−4	6224.752748	−0.0158(14)	−0.0177(7)	−0.0179(5)	−0.0195(7)	−0.0197(5)	−0.0191	−0.0508
−2	6226.348676	−0.0237(21)	−0.0287(7)	−0.0264(1)	−0.0312(7)	−0.0287(1)	−0.0323	−0.0729
1	6228.689985	0.0305(18)	0.0395(4)	0.038(12)	0.0415(4)	0.0398(12)	0.0433	0.0764
3	6230.215765	0.0236(14)	0.0226(8)	0.0221(3)	0.0252(8)	0.0247(3)	0.0268	0.0659
5	6231.713422	0.0171(23)	0.0163(8)	0.0174(4)	0.0161(8)	0.0172(4)	0.0186	0.0476
7	6233.182896	0.0130(18)	0.0126(5)	0.0124(5)	0.0127(5)	0.0124(5)	0.0123	0.0318
9	6234.624116	0.0078(8)	0.0066(3)	0.0061(5)	0.0080(3)	0.0074(5)	0.0075	0.0193
11	6236.036992	0.0063(3)	0.0050(8)	0.0045(4)	0.0042(8)	0.0038(4)	0.0038	0.0096
13	6237.421424	0.0032(2)	0.0019(6)	0.0019(5)	0.0015(6)	0.0015(5)	0.0008	0.0023
15	6238.777296	0.0016(1)	0.0013(5)	0.0012(4)	−0.0008(5)	−0.0008(4)	−0.0017	−0.0033
17	6240.104478	0.0002(1)	−0.0020(4)	−0.0021(10)	−0.0028(4)	−0.0029(10)	−0.0039	−0.0075
19	6241.402828	−0.0010(1)	−0.0031(8)	−0.0032(13)	−0.0043(8)	−0.0045(13)	−0.0057	−0.0109
21	6242.672191	−0.0023(3)	−0.0045(6)	−0.0048(6)	−0.0059(6)	−0.0064(6)	−0.0073	−0.0137
23	6243.912398	−0.0033(3)	−0.0056(5)	−0.0056(5)	−0.0068(5)	−0.0067(5)	−0.0087	−0.0161
25	6245.123271	−0.0045(5)	−0.0063(2)	−0.0064(2)	−0.0096(2)	−0.0097(2)	−0.0100	−0.0182
27	6246.304618	−0.0054(4)	−0.0083(4)	−0.0088(4)	−0.0095(4)	−0.0108(4)	−0.0112	−0.0201
29	6247.456239	−0.0061(6)	−0.0077(3)	−0.0085(3)	−0.0119(3)	−0.0131(3)	−0.0122	−0.0218
31	6248.577920	−0.0068(5)	−0.0104(8)	−0.0096(3)	−0.0109(8)	−0.0110(3)	−0.0132	−0.0233
33	6249.669442	−0.0070(10)	−0.0103(8)	−0.0102(6)	−0.0106(8)	−0.0105(6)	−0.0142	−0.0247
35	6250.730575	−0.0075(7)	−0.0102(5)	−0.0094(16)	−0.0133(5)	−0.0124(16)	−0.0150	−0.0260
37	6251.761081	−0.0090(6)	−0.0132(3)	−0.0125(4)	−0.0159(3)	−0.0151(4)	−0.0159	−0.0272
39	6252.760717	−0.0090(6)	−0.0136(7)	−0.0137(8)	−0.0166(7)	−0.0168(8)	−0.0167	−0.0282
41	6253.729232	−0.0090(9)	−0.0145(6)	−0.0135(23)	−0.0139(6)	−0.0129(23)	−0.0175	−0.0292
43	6254.666372	−0.0102(12)	−0.0120(8)	−0.0127(14)	−0.0162(8)	−0.0172(14)	−0.0183	−0.0301
45	6255.571877	−0.0099(10)	−0.0142(3)	−0.0146(21)	−0.0154(3)	−0.0159(21)	−0.0191	−0.0308
47	6256.445485	−0.0109(9)	−0.0178(6)	−0.0166(27)	−0.0191(6)	−0.0178(27)	−0.0199	−0.0315
49	6257.286932	−0.0115(9)	−0.0164(4)	−0.018(16)	−0.0188(4)	−0.0207(16)	−0.0207	−0.0321
51	6258.095953	−0.0110(8)	−0.0181(3)	−0.0176(3)	−0.0218(3)	−0.0211(3)	−0.0216	−0.0327
53	6258.872284	−0.0120(12)	−0.0177(2)	−0.0188(2)	−0.0229(2)	−0.0243(2)	−0.0225	−0.0332
55	6259.615664		−0.0180(0)	−0.0197(0)	−0.0184(0)	−0.0203(0)	−0.0234	−0.0336

The coefficients listed for 217 K were calculated using the exponential power gap (EPG) scaling law, energy corrected sudden model (ECS) and their temperature dependence coefficients from Ref. [17].

[a] Line positions are from HITRAN2008 [16].

Table 6
Self line mixing coefficients in the 30012←00001 band of carbon dioxide.

m	Position[a] (cm^{-1})	Y(296 K) (atm^{-1}) [4]	Y(258 K) (atm^{-1})		Y(235 K) (atm^{-1})		Y(217 K) (atm^{-1})	
		SDV	VOIGT	SDV	VOIGT	SDV	EPG	ECS
−56	6292.996793	0.0057(7)	0.0076(7)	0.0083(7)	0.0086(7)	0.0078(8)	0.0087	0.0118
−54	6295.319763	0.0059(6)	0.0063(6)	0.007(6)	0.0071(6)	0.0061(6)	0.0088	0.0123
−52	6297.618698	0.0057(7)	0.0078(7)	0.0083(7)	0.0088(7)	0.0085(9)	0.0089	0.0127
−50	6299.893141	0.0051(4)	0.0065(4)	0.0062(4)	0.0074(4)	0.006(6)	0.0090	0.0132
−48	6302.142653	0.0052(8)	0.0084(9)	0.009(9)	0.0095(9)	0.0085(6)	0.0091	0.0136
−46	6304.366820	0.0071(9)	0.0065(9)	0.0063(9)	0.0074(9)	0.0066(5)	0.0091	0.0140
−44	6306.565247	0.0077(3)	0.0081(3)	0.0086(3)	0.0092(3)	0.0088(9)	0.0092	0.0143
−42	6308.737560	0.0073(3)	0.0075(3)	0.0072(3)	0.0086(3)	0.0068(7)	0.0092	0.0146
−40	6310.883410	0.0046(7)	0.0074(7)	0.0069(7)	0.0085(7)	0.0074(8)	0.0093	0.0148
−38	6313.002450	0.0067(4)	0.0075(4)	0.0068(3)	0.0086(4)	0.0078(8)	0.0093	0.0150
−36	6315.094370	0.0059(3)	0.007(3)	0.0076(3)	0.0081(3)	0.0067(7)	0.0092	0.0151
−34	6317.158870	0.0079(3)	0.0079(3)	0.0080(3)	0.0092(3)	0.0083(9)	0.0091	0.0151
−32	6319.195680	0.0065(6)	0.007(5)	0.0068(6)	0.0081(5)	0.0071(8)	0.0090	0.0150
−30	6321.204520	0.0046(3)	0.007(3)	0.0064(3)	0.0082(3)	0.0074(8)	0.0088	0.0148
−28	6323.185160	0.0046(3)	0.0058(3)	0.0059(3)	0.0068(3)	0.0058(6)	0.0086	0.0145
−26	6325.137350	0.0048(4)	0.0058(4)	0.0056(4)	0.0069(4)	0.0056(6)	0.0082	0.0140
−24	6327.060900	0.0035(3)	0.0055(3)	0.0050(3)	0.0066(3)	0.0055(6)	0.0078	0.0133
−22	6328.955590	0.0034(3)	0.0058(3)	0.0062(4)	0.0070(3)	0.0061(7)	0.0072	0.0124
−20	6330.821240	0.0028(4)	0.0044(3)	0.0043(3)	0.0054(3)	0.0043(5)	0.0064	0.0111
−18	6332.657690	0.0025(3)	0.0034(3)	0.0038(3)	0.0043(3)	0.0032(4)	0.0055	0.0092
−16	6334.464790	0.0012(3)	0.0025(3)	0.0025(3)	0.0033(3)	0.0027(3)	0.0043	0.0067
−14	6336.242380	−0.0005(4)	0.0011(4)	0.0010(3)	0.0018(4)	0.0010(1)	0.0027	0.0030
−12	6337.990360	−0.0019(4)	−0.0005(4)	−0.0005(3)	0.0001(4)	−0.0005(1)	0.0006	−0.0021
−10	6339.708600	−0.0041(3)	−0.0029(3)	−0.0028(3)	−0.0026(3)	−0.0026(3)	−0.0021	−0.0094
−8	6341.397010	−0.0076(4)	−0.0054(4)	−0.0055(4)	−0.0053(4)	−0.0050(5)	−0.0057	−0.0194
−6	6343.055515	−0.0117(5)	−0.0088(5)	−0.0093(5)	−0.0092(5)	−0.0081(8)	−0.0109	−0.0331
−4	6344.684033	−0.0152(1)	−0.0184(1)	−0.0199(1)	−0.0197(1)	−0.0173(8)	−0.0187	−0.0510
−2	6346.282512	−0.0366(12)	−0.0307(12)	−0.0283(12)	−0.0334(12)	−0.0317(7)	−0.0321	−0.0740
1	6348.623821	0.0735(1)	0.0414(3)	0.041(2)	0.0454(3)	0.0456(5)	0.0452	0.0802
3	6350.147049	0.0285(8)	0.0264(4)	0.0277(4)	0.0285(4)	0.0261(8)	0.0268	0.0684
5	6351.640150	0.0224(5)	0.0172(5)	0.0177(5)	0.0182(5)	0.0163(7)	0.0184	0.0486
7	6353.103127	0.0139(5)	0.0104(5)	0.0097(5)	0.0108(5)	0.011(11)	0.0120	0.0319
9	6354.535999	0.0077(4)	0.0077(4)	0.0082(4)	0.0077(4)	0.0075(7)	0.0072	0.0187
11	6355.938798	0.0052(5)	0.0041(5)	0.0044(5)	0.0037(5)	0.0038(3)	0.0035	0.0088
13	6357.311571	0.0039(4)	0.0018(4)	0.0018(3)	0.0012(4)	0.0018(10)	0.0005	0.0014
15	6358.654375	0.0024(10)	−0.0003(10)	−0.0003(11)	−0.0013(10)	−0.0003(12)	−0.0020	−0.0041
17	6359.967287	0.0004(13)	−0.0022(12)	−0.0022(13)	−0.0034(12)	−0.0024(7)	−0.0041	−0.0084
19	6361.250392	−0.0036(6)	−0.0041(6)	−0.0037(5)	−0.0055(6)	−0.0045(10)	−0.0060	−0.0117
21	6362.503794	−0.0027(5)	−0.0056(4)	−0.0057(5)	−0.0071(4)	−0.0056(7)	−0.0076	−0.0144
23	6363.727610	−0.0032(2)	−0.0067(2)	−0.0069(2)	−0.0083(2)	−0.0066(8)	−0.0090	−0.0168
25	6364.921972	−0.0036(4)	−0.0081(4)	−0.0073(4)	−0.0099(4)	−0.0086(10)	−0.0103	−0.0188
27	6366.087029	−0.0062(3)	−0.0094(3)	−0.0096(3)	−0.0113(3)	−0.0102(12)	−0.0115	−0.0207
29	6367.222942	−0.0072(3)	−0.0086(3)	−0.0091(3)	−0.0103(3)	−0.0091(10)	−0.0126	−0.0224
31	6368.329891	−0.0079(6)	−0.0097(6)	−0.0094(6)	−0.0115(6)	−0.0092(11)	−0.0136	−0.0239
33	6369.408072	−0.0091(16)	−0.0103(16)	−0.0109(16)	−0.0121(16)	−0.0112(12)	−0.0146	−0.0252
35	6370.457697	−0.0085(5)	−0.0107(4)	−0.0100(5)	−0.0125(4)	−0.0106(12)	−0.0155	−0.0265
37	6371.478995	−0.0097(8)	−0.0116(8)	−0.0109(8)	−0.0135(8)	−0.0124(11)	−0.0164	−0.0276
39	6372.472214	−0.0101(22)	−0.0112(23)	−0.0103(22)	−0.0130(23)	−0.0111(12)	−0.0172	−0.0285
41	6373.437620	−0.0083(14)	−0.0143(14)	−0.0130(14)	−0.0166(14)	−0.0136(11)	−0.0180	−0.0294
43	6374.375495	−0.0103(21)	−0.0167(20)	−0.0153(22)	−0.0192(20)	−0.0158(13)	−0.0188	−0.0301
45	6375.286144	−0.0097(26)	−0.0156(27)	−0.0154(26)	−0.0179(27)	−0.0140(11)	−0.0196	−0.0307
47	6376.169890	−0.0099(17)	−0.0155(16)	−0.0164(18)	−0.0178(16)	−0.0147(11)	−0.0203	−0.0312
49	6377.027075	−0.0128(9)	−0.0193(19)	−0.0208(27)	−0.0221(19)	−0.0174(13)	−0.0211	−0.0316
51	6377.858065	−0.0140(7)	−0.0171(19)	−0.0178(30)	−0.0196(19)	−0.0171(12)	−0.0218	−0.0319
53	6378.663244	−0.0152(6)	−0.0169(19)	−0.0167(2)	−0.0192(19)	−0.0160(13)	−0.0226	−0.0322
55	6379.443023	−0.0166(7)	−0.0172(0)	−0.0166(0)	−0.0195(0)	−0.0168(11)	−0.0234	−0.0323

The coefficient ts listed for the 217 K temperature were calculated using the exponential power gap (EPG) scaling law, energy corrected sudden model (ECS) and their temperature dependence coefficients from Ref. [17].

[a] Line positions are from HITRAN2008 [16].

The self-line mixing coefficients calculated using the ECS model followed the "fit 1" procedure described in Ref. [17], that takes into account the temperature dependence of the parameters $A(T)$ and $d_c(T)$ from the basic rates and adiabatic factor, respectively, as described in Eqs. (10)–(12) of Ref. [17]. The self line mixing coefficients were calculated using the values of the temperature dependence coefficient "N1" and "N2" of the $A(T)$ and

$d_c(T)$ parameters in Eq. (12) of Ref. [17] and Tables 7A and B of Ref. [17]. The room temperature values of the adjustable parameters for self-broadened transitions were taken from Table 5 of Ref. [17].

All results are plotted against m (or $|m|$). In both figures the top panel presents results in the 30013←00001 band and the bottom panel presents our results for the 30012←00001 band. Both fitting laws used successfully modeled the entire range of rotational states. However, none of them fits perfectly the measured broadening parameters. For $|m|$ values between 10 and 35 both models provide a good agreement with the experimental results. The ECS model fails to reproduce well the measurements at very low $|m|$, whereas the EPG model seems to overestimate the broadening for $|m|>17$. For the line mixing coefficients the EPG model seems to give an overall better agreement than the ECS model. However, as pointed in Refs. [4,17], none of these models reproduce the self-broadening coefficients very well over the entire range of $|m|$ values.

An inspection of the experimental and calculated line mixing results plotted in panels A–C of Figs. 5 and 6, shows that the ECS model does not reproduce well the measured line mixing results, especially at very low and high $|m|$. Overall, the EPG and ECS fitting laws modeled the entire range of $|m|$, but they did not fit very well the observed self-line mixing coefficients at 296, 258 and 235 K.

5. Conclusion

In this study we have measured for the first time the temperature dependences of self-broadened line parameters using a set of 46 spectra of pure carbon dioxide in the 30013←00001 and 30012←00001 bands recorded at 296, 258, 235 and 217 K. A multispectrum fit technique was used in the analysis. The line profiles were fitted using the Voigt and speed dependent Voigt line shape models that incorporated line mixing and speed dependence.

Semiclassical theoretical calculations of the self-broadened half widths were performed using the Robert–Bonamy formalism [13] and used to calculate theoretical temperature dependence coefficients for the self-broadening coefficients. The calculated self-broadened half widths were found to be in good agreement (within a few percent) with the corresponding measured self-broadened widths. The agreement of the calculated temperature dependence coefficients with the measured values is very good.

The measured values for the temperature dependent coefficients in self-broadened CO_2 pressure shifts did not show a dependence on $|m|$. A similar observation was made in our study of CO_2 and air mixtures [12]. One observable difference is the fact that the average value for δ' in pure CO_2 is about $0.000077\,cm^{-1}\,atm^{-1}\,K^{-1}$, different from the value of $-0.00006\,cm^{-1}\,atm^{-1}\,K^{-1}$ obtained for air-broadened spectra.

We were able to quantify the line mixing effects in pure carbon dioxide only at room temperature [4], 258 and 235 K. The line mixing coefficients were modeled using parameters for their temperature dependences reported in our study in Ref. [17]. At both very low and high $|m|$ values the Energy Corrected Sudden (ECS) model failed to reproduce the measurements very well whereas for the line mixing coefficients the Exponential Power Gap (EPG) model seems to give a slightly better agreement. The results presented in this paper will improve our general understanding of the pressure broadening and pressure-shift parameters and line mixing effects in self-broadened carbon dioxide.

Acknowledgments

A. Predoi-Cross and A.R.W. McKellar are grateful for financial support from the National Sciences and Engineering Research Council of Canada. R.R. Gamache and A.L. Laraia are pleased to acknowledge support of this research by the National Science Foundation through Grant no. ATM-0803135. Any opinions, findings, and conclusions or recommendations expressed in this material are those of the author(s) and do not necessarily reflect the views of the National Science Foundation.

References

[1] Toth RA, Brown LR, Miller CE, Malathy Devi V, Benner DC. Spectroscopic database of CO_2 line parameters: 4300–7000 cm^{-1}. J Quant Spectrosc Radiat Transfer 2008;109:906–21.
[2] Malathy Devi V, Benner DC, Brown LR, Miller CE, Toth RA. Line mixing and speed dependence in CO_2 at 6348 cm^{-1}: positions, intensities, and air- and self-broadening derived with constrained multispectrum analysis. J Mol Spectrosc 2007;242:90–117.
[3] Malathy Devi V, Benner DC, Brown LR, Miller CE, Toth RA. Line mixing and speed dependence in CO_2 at 6227.9 cm^{-1}: constrained multispectrum analysis of intensities and line shapes in the 30013←00001 band. J Mol Spectrosc 2007;245:52–80.
[4] Predoi-Cross A, Unni AV, Liu W, Schofield I, Holladay C, McKellar ARW, et al. Line shape parameters measurement and computations for self-broadened carbon dioxide transitions in the 30012←00001 and 30013←00001 bands, line mixing, and speed dependence. J Mol Spectrosc 2007;245:34–51.
[5] Suarez CB, Valero FPJ. Absolute intensity measurements at different temperatures of the $^{12}C^{16}O_2$ bands $30^{\circ}1_I \leftarrow 00^00$ and $30^{\circ}1_{IV} \leftarrow 00^00$. J Quant Spectrosc Radiat Transfer 1978;19:569–78.
[6] Valero FPJ, Suarez CB. J. Measurement at different temperatures of absolute intensities, line half-widths, and broadening by Ar and N_2 for the $30^01_{II} \leftarrow 00^00$ band of CO_2. J Quant Spectrosc Radiat Transfer 1978;19:579–90.
[7] Tettemer GL, Planet WG. Intensities and pressure-broadened widths of CO_2 R-branch lines at 15 μm from tunable laser measurements. J Quant Spectrosc Radiat Transfer 1980;24:343–5.
[8] Margottin-Maclou M, Dahoo P, Henry A, Valentin A, Henry L. Self-, N_2-, and O_2-broadening parameters in the ν_3 and $\nu_1+\nu_3$ bands of $^{12}C^{16}O_2$. J Mol Spectrosc 1988;131:21–35.
[9] Varanasi P. Infrared line widths at planetary atmospheric temperatures. J Quant Spectrosc Radiat Transfer 1988;39(1):13–25.
[10] Aushev AF, Borisova NF, Bykova ES, Osipov VM, Tsukanov VV. On the temperature dependence of spectral line half width for CO_2 and H_2O. Opt Spektrosk 1990;68(5):1197–9.
[11] Arshinov KI, Leshenyuk NS. Temperature dependence of the collisional broadening of laser lines of the CO_2 molecule. Quant Electron 1997;27(6):503–4.
[12] Predoi-Cross A, McKellar ARW, Benner DC, Malathy Devi V, Gamache RR, Miller CE, et al. Temperature dependences for air-broadened Lorentz half-width and pressure shift coefficients in the 30013←00001 and 30012←00001 bands of CO_2 near 1600 nm. Can J Phys 2009;87:517–35.
[13] Robert D, Bonamy J. Short-range force effects in semi-classical molecular line broadening calculations. J de Phys 1979;40:923–43.

[14] Hurtmans D, Dufour G, Bell W, Henry A, Valentin A, Camy-Peyret C. Line Intensity of R(0) and R(3) of the $^{12}CH_4$ $2\nu_3$ band from diode laser spectroscopy. J Mol Spectrosc 2002;215:128–33.
[15] Rothman LS, Jacquemart D, Barbe A, Benner DC, Birk M, Brown LR, et al. The HITRAN 2004 molecular spectroscopic database. J Quant Spectrosc Radiat Transfer 2005;96:139–204.
[16] Rothman LS, Gordon IE, Barbe A, Benner DC, Bernath PF, Birk M, et al. The HITRAN 2008 molecular spectroscopic database. J Quant Spectrosc Radiat Transfer 2009;110:533–72.
[17] Povey C, Predoi-Cross A. Computations of temperature dependences for line shape parameters in the 30012←00001 and 30013←00001 bands of pure CO_2. J Mol Spectrosc 2009;257: 187–99.
[18] Baranger M. General impact theory of pressure broadening. Phys Rev 1958;112:855–65.
[19] Ben-Reuven A. Spectral line shapes in gases in the binary-collision approximation. In: Prigogine I, Rice SA, editors. Advances in chemical physics. New York: Academic Press; 1975. p. 235.
[20] Sack RA. Two-center expansion for the powers of the distance between two points. J Math Phys 1964;5:260–8.
[21] Rosenmann L, Hartmann J-M, Perrin MY, Taine J. Collisional broadening of CO_2 IR lines. II. Calculations. J Chem Phys 1988;88: 2999.
[22] Rothman LS, Hawkins RL, Wattson RB, Gamache RR. Energy Levels, intensities, and linewidths of atmospheric carbon dioxide bands. J Quant Spectrosc Radiat Transfer 1992;48:537–66.
[23] Diaz Pena M, Pando C, Renuncio JAR. Combination rules for intermolecular potential parameters. I. Rules based on approximations for the long-range dispersion energy. J Chem Phys 1982;76: 325–32.
[24] Diaz Pena M, Pando C, Renuncio JAR. Combination rules for intermolecular potential parameters. II. Rules based on approximations for the long-range dispersion energy and an atomic distortion model for the repulsive interaction. J Chem Phys 1982;76:333–9.
[25] Good RJ, Hope CJ. Test of combining rules for intermolecular distances. Potential function constants from second virial coefficients. J Chem Phys 1971;55:111–6.
[26] Hirschfelder JO, Curtis CF, Bird RB. Molecular theory of gases and liquids. New York: Wiley; 1964.
[27] Gamache RR, Fischer J. Half-widths of $H_2^{16}O$, $H_2^{18}O$, $H_2^{17}O$, $HD^{16}O$, and $D_2^{16}O$: I. Comparison between isotopomers. J Quant Spectrosc Radiat Transfer 2003;78:289–304.
[28] Gamache RR. Line shape parameters for water vapor in the 3.2 to 17.76 μm region for atmospheric applications. J Mol Spectrosc 2005;229:9–18.
[29] Gamache RR, Hartmann J-M. Collisional parameters of H_2O lines: effects of vibration. J Quant Spectrosc Radiat Transfer 2004;83: 119–47.
[30] Birnbaum G. Microwave pressure broadening and its application to intermolecular forces. Adv Chem. Phys. 1967;12:487–548.
[31] Hartmann J-M, Taine J, Bonamy J, Labani B, Robert D. Collisional broadening of rotation-vibration lines for asymmetric-top molecules. II. H_2O diode laser measurements in the 400–900 K range; calculations in the 300–2000 K range. J Chem Phys 1987;86: 144–56.
[32] Wagner G, Birk M, Gamache RR, Hartmann J-M. Collisional parameters of H_2O lines: effect of temperature. J Quant Spectrosc Radiat Transfer 2005;92:211–30.
[33] Toth RA, Brown LR, Smith MAH, Malathy Devi V, Benner DC, Dulick M. Air-broadening of H_2O as a function of temperature: 696–2163 cm^{-1}. J Quant Spectrosc Radiat Transfer 2006;101: 339–66.
[34] Gamache RR, Laraia AL. N_2-, O_2-, and air-broadened half-widths, their temperature dependence, and line shifts for the rotation band of $H_2^{16}O$. J Mol Spectrosc 2009;257:116–27.
[35] Gamache RR, Arié R, Boursier C, Hartmann J-M. A review of pressure-broadening and pressure-shifting of spectral lines of ozone. Spectrochim Acta A 1998;54:35–63.